The Segmentation of Nuclei in Digital Pathology in microscopic Images

Mr. Tojo Mathew
Assistant Professor, Dept. of CSE
National Institute of Engineering, Mysuru

Nandan, Puneeth Keerthan, Saiprashanth Budadinne, Sharana Basava
Computer Science and Engineering,
National Institute of Engineering, Mysuru

Abstract

We propose a method for segmentation of cancer nuclei which conflicts to the normal nuclei which involve indicative of brain tumors pathologically in microscopic images. To constrain the problem the spaces in the region of color information first we begin by converting the images into the V component of HSV (Hue, Saturation, Value)we are using the level-set segmentation in the training stage, next we follow by applying the sparsity representation (SR) in the test stage. In the process in SR, the proposed system VLS-SR will improve the capability of searching recursively for the optimal threshold level-set in the working subsets of the SR where the image cancer nuclei segmentation.

Index Terms- *Microscopy images, digital pathology, histopathology, nucleus, cell, detection, segmentation, Annotation, boundaries, dataset, deep learning, nuclear segmentation, nuclei..*

1.INTRODUCTION

In huge increasing threat in low and middle-income countries. Brain tumors in normal occupy the 14th place infrequency of all cancers, and due to their particularly poor diagnosis they are the sixth most common cause of cancer death in the under 65-year-old population. In addition, they are the second most common cancer in children and the most common cause of cancer death in children. It is evident that the chance of survival can be increased if the brain tumor is detected correctly at its early stage. Thus, there is a need for efficient medical image segmentation methods with very preferred properties with very fast computation and very robust results. Image segmentation refers to the partitioning of an image into forming disjoint regions with form to a chosen property such as texture and color. As the tissue segmentation which is formed early in clinical decision support. In the image segmentation stage, many methods relied on the preprocessing steps for the task of brain tissue classification. Alternatively, another popular category of brain tissue segmentation methods is based on utilizing geometric information such as deformable models using a minimization of an energy functional. However, the deformable models required appropriate parameter settings and considerably complex pre-processing steps in brain tissue segmentation.

2.PROPOSED FRAMEWORK

Many challenges for microscopic image cancer nuclei segmentation in clinical support systems for brain tumor diagnosis. There could be more importance of multifaceted components in the design of hybrid approaches to image pattern segmentation. The sparsity techniques have been explored for the image shape modeling and compressed sensing using the adaptive framework of wavelet packets . Conversion of a color image is very common in digital transformation is widely used in image analysis for segmentation purpose. In this study, we propose an automatic method, as illustrated in Figure 1, for segmentation of cancer nuclei when such conflicts of cancer nuclei involve ‘omics’ indicative of brain tumors pathologically. To constrain the problem space in the region of color information, we begin by converting the images into the V component using the level-set segmentation (VLS) in the training stage, follow by applying the sparsity representation (SR) in the test stage.

A. The Training Stage in VLS

In the approach, based on the microscopic image conversion in the V component, the model of VLS is performed only the search direction, in the subsets of bin ranges ,n the histogram. Let r (*k*) let be the average value of a lower threshold Lt(*k*) and an let the upper threshold Ut (*k*). At the *k*th iteration, the Lt(*k*) and Ut(*k*) are thus represented by

$$\mathrm{Lt}(k) = \mathrm{r}(k+1) - \frac{\{1-\mathrm{r}(k+1)\}}{2},$$
$$\text{and } \mathrm{Ut}(k) = \mathrm{r}(k+1) + \frac{\{1-\mathrm{r}(k+1)\}}{2}. \quad (1)$$

The denote the term of x_k as a binary range at the *k*th iteration, technique, We define the propagation direction S*k* the search directionin the sparsity fixed by the Lt(*k*) and Ut(*k*) in the histogram value in the V at a given subset of x_k, g(x_k) be the intensity.

$$\text{if } \mathrm{g}(x_k) < \frac{\mathrm{Ut}(k) - \mathrm{Lt}(k)}{2} + \mathrm{Lt}(k), \quad \mathrm{S}_k = \mathrm{g}(x_k) - \mathrm{Lt}(k);$$
$$\text{otherwise}, \quad \mathrm{S}_k = \mathrm{Ut}(k) - \mathrm{g}(x_k). \quad (2)$$

B. The Test Stage of SR

The working of the details of the sparsity technique can be found in, we are using the active-set method to define the search direction S_k (at the *k*th iteration) inthe working subsets. The active-set method one of the most popular methods for the constrained problems is, which maintains a population of individuals with pre-defined working subsets. (*k* + 1)th iteration, the working subset of x_{k+1} is formulated as S ,

$$x_{k+1} = x_k + \alpha \times \mathrm{S}_k,$$

$x_k\,(x_k \in \mathbf{X})$ is a bin range which is fixed by the bounds with two thresholds, an upper threshold U t(*k*) a lower threshold L t(*k*) and at the *k*th iteration. Tone important consideration for the design of object function is to ensure that the measurement procedure
gives the segmentation evaluation for the samples, he working subsets induce a partition of *xk* into a set of fixed bin ranges in the greyscale histogram ,regardless of the coordinate system for the mapped data in the histograms.

$$\underset{x_k \in \mathbf{X}}{\text{minimize}}\ \mathrm{D}(k) = |\mathrm{T}(x_k) - \tau|, \quad \text{with } \mathrm{Lt}(k) \le x_k \le \mathrm{Ut}(k),$$

C. *Stained Images of Hematoxylin and Eosin*

Due to its low cost, widespread use for primary diagnosis, and potential for use in highly predictive models, our dataset covers H&E stained images Histologic structure of a tissue primarily consists of epithelium , lumen, adipose,and stroma. Shape, size, color, and crowding of glands, as well as various nuclei in epithelium and stroma reveal a lot of information about the health of the tissue to a pathologist. The combination of hematoxylin and eosin, or H&E, is a unclear, general, and inexpensive staining scheme. Hematoxylin renders nuclei dark blueish purple and epithelium light purple, while eosin renders stroma pink. Together, H&E enhance the contrast between nuclei, epithelium, and stroma for examination under a microscope. There seems to be a vast amount of untapped information in H&E stained images that can be used for specific diagnoses such as cancer molecular sub-types determination, mortality prediction , and treatment effectiveness prediction .. However, most machine learning techniques can easily be trained on tissue images with other types of stains.

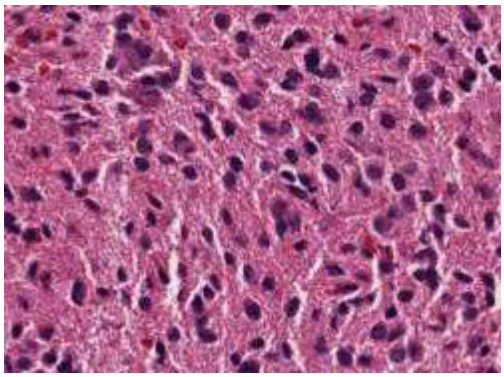

Fig- A sample image

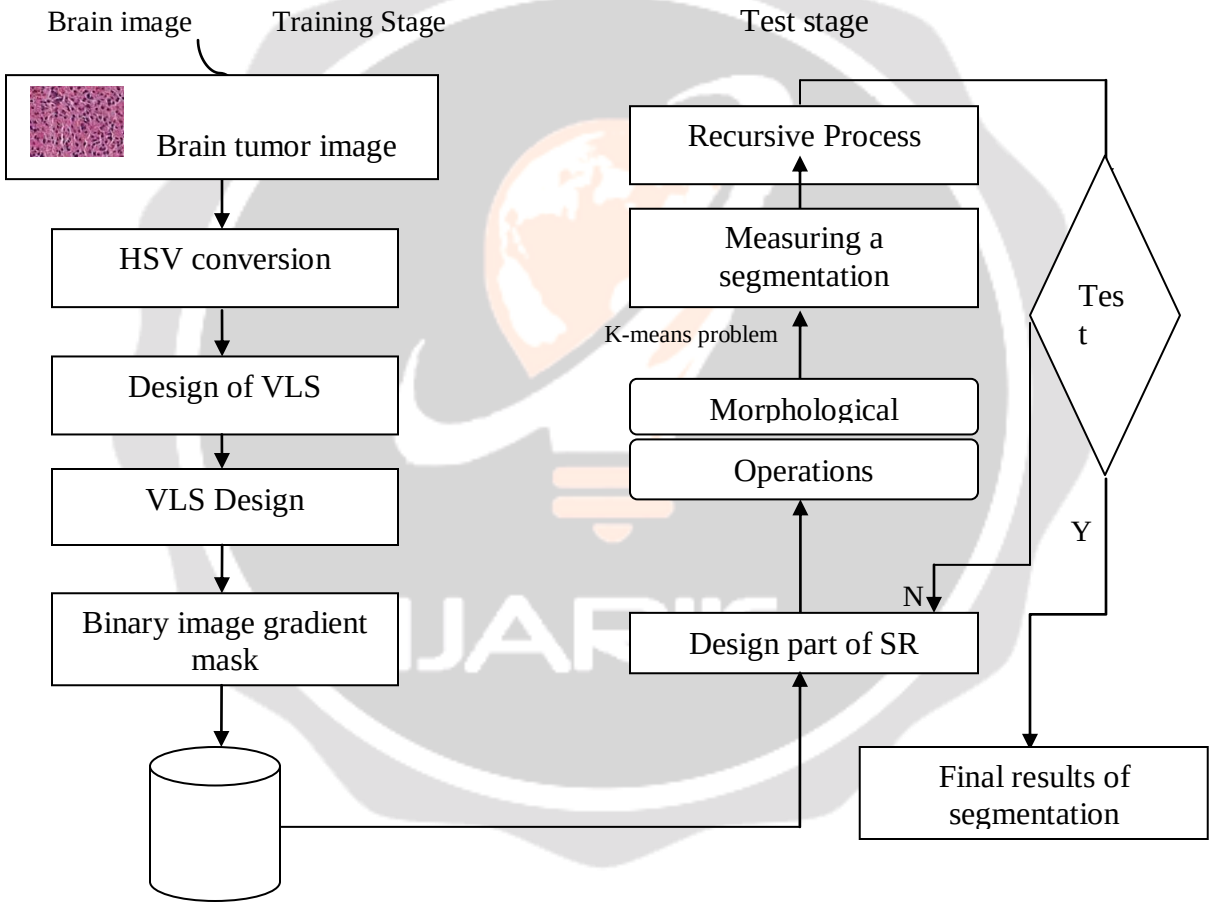

FIGURE: PROPOSED SYTEM

Cropped versions of the seven test images, one for each organ, are shown , including three from the organs not used for training. These images demonstrate the variation in the tissue and nuclear appearances represented in our dataset., and were not used for producing test segmentation. The ideal inside and outside class maps are easy to infer and have been omitted. illustrates how color normalization reduces appearance variability of H&E stains . R shows the estimated boundary. We willagain omit showing maps for the other two classes. Finally, the segmented nuclei micro images maps are shown in as bin-ary masks to observe which nuclei were merged or unnecessarily split and which were not. It is clear that even the crowded and chromatinsparse nuclei were correctly segmented using. The generalization power of the proposed methodis demonstrated by testing on unseen patients and multiple organs, including some unseen organs.

3. ANNOTATED DATASET

It is a time consuming task to find, download, and annotating tissue slides , which may impede the development of new nuclear segmentation software that can be used in computational pathology. We hosted data set with a diverse set of tissue images and painstakingly annotated nuclear boundaries can fill this gap. Can used by the research community to develop and benchmark generalized nuclear segmentation techniques that work on diverse nuclear types. Our dataset consists of one of most the commonly used images – H&E stained and captured at 40x magnification. Although we used H&E stained tissue slides digitized at 41x magnification for developing the proposed algorithm, but our approach can be easily applied to the commonly available 20x slides by re-training or appropriate up sampling to 40x using super-resolution techniques tailored for such images and used only one WSI per patient to maximize nuclear appearance variation. These images came from 18 different hospitals, which introduced another source of appearance variation due to the differences in the staining practices across labs.

Since computational requirements for processing are high, we have cropped sub-images of size 100×100 from regions of the dense in nuclei, keeping only two such cropped image per and patient. To enrich, ensure richness of nuclear appearances, we covered six different organs, liver, kidney, prostate, bladder, colon and stomach. After obtaining 100 × 100 sub-images, we annotated more than 20,000 nuclear boundaries Images were enlarged to 200× on a 24" monitor such that each image pixel occupied 5 × 5 screen pixels for clear visibility, and the nuclear boundaries were annotated with a laser mouse. The annotators were engineering students, and were trained to identify nuclear boundaries by us. For overlapping nuclei, we assigned each multi-nuclear pixel to the largest nucleus containing that pixel, and the composition of the dataset is shown

We sent annotated images to an expert pathologist for examination of annotation quality, we used one image per slide. On a slide, we put the unannotated and annotated images side by side to cover a large portion of the slide. The pathologist viewed the slide on a 25" monitor, and was instructed to place an arrow shape on every problematic annotation, whether it was a false positive, a false negative, an over-segmented, or an under-segmented nucleus. We counted all the arrows and divided the count by the number of annotated nuclei in those images to estimate that our annotators made less than 1.5% errors on any given image. We left these errors uncorrected due to their low count

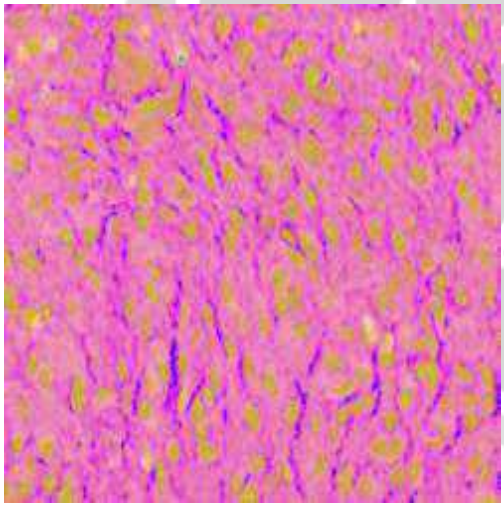

Figure 3. Image conversion in HSV color space of HSV with the sampleimage

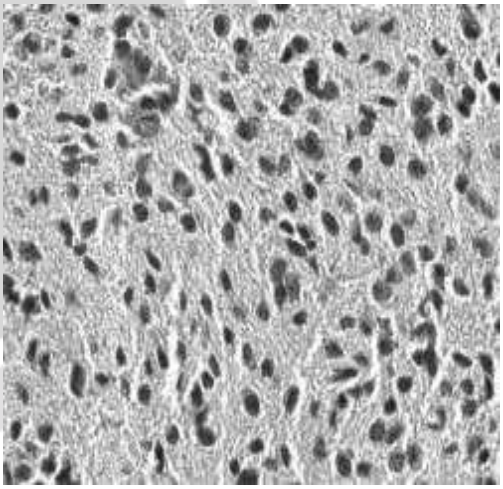

Figure 4. transformed image in the V component with the sample image

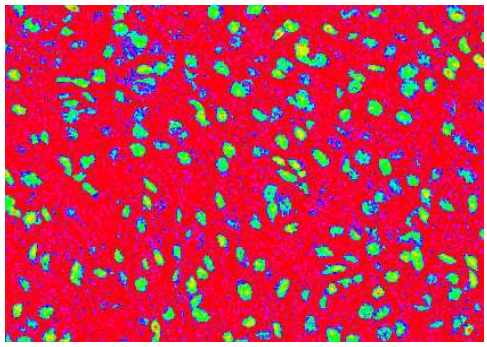

Figure 5: the VLS representation with segmented sample image output in the region of V = (0.08, 0.67).

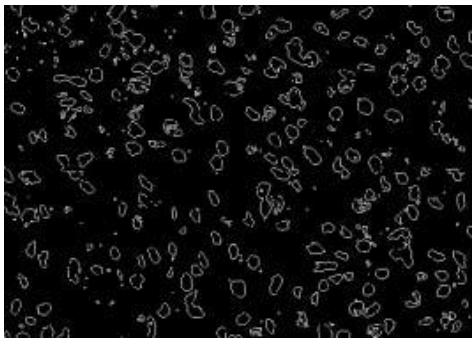

Figure 6. Out put of segmented sample image in portraying before imag segmentation.

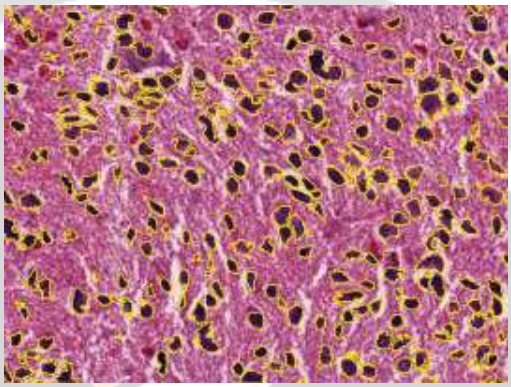

Figure: Resulting segmented image

4.CONCLUSION

We propose a new method for segmentation of cancer nuclei when such conflicts of cancer nuclei involve 'omics' indicative of brain tumors pathologically. To study the problem space in the region of color information, in the training stage we start by converting the images into the V component of the HSV color space using the level-set segmentation, in test stage to applying the sparsity technique.

The proposed method provides an improved capability of searching brain tumors recursively for the optimal level-set in the working subsets for image cancer nuclei segmentation. In the validation stage, the proposed system shows the quantitative segmentation accuracies in segmentation of cancer nuclei on the CBTC dataset.

In future work will be focused on establishing the robustness of the proposed method for quantitative analysis of the characteristics of cancer nuclei pathologically in the brain tumor detection.

REFERENCES

[1] Anbeek P, Vincken KL, van Osch MJ, Bisschops RH, van der Grond J. Probabilistic segmentation of white matter lesions in MR imaging. *Neuroimage* 21, pp. 1037–1044, 2004.

[2] Aharon, M., Elad, M. and Bruckstein, A. An algorithm for designing overcomplete dictionaries for sparse representation. IEEE Transactions on Signal Processing, 4311- 4322, 2006.

[3] Bagcı, U., Bray, M., Caban, J., Yao, J., Mollura, D. J. Computerassisted detection of infectious lung diseases: a review. Computerized Medical Imaging and Graphics, vol. 36, pp. 72-84, 2012.

[4] Computational Brain Tumor Cluster of Event (CBTC), 'Challenge 1 Segmentation of Nuclei in Digital Pathology Images', MICCAI, Munich, Germany, 2015.

[5] Doi, K. Computer-aided diagnosis in medical imaging: historical review, current status and future potential. Computerized Medical Imaging and Graphics, vol. 31, pp. 198-211, 2007.

[6] Duchesne, S., Caroli, A., Geroldi, C., Barillot, C., Frisoni, G.B., Collins, D.L. MRI based automated computer classification of probable ad versus normal controls. IEEE Trans. Med. Imaging 27, pp. 509–520, 2008.

[7] El-Zehiry Y. N. and Elmaghraby A. Brain MRI tissue classification using graph cut optimization of the mumford-shah functional. Proc. of Image and Vision Computing, pp. 321–326, 2007.

[8]Huang A., Abugharbieh R., R. Tam R. A Hybrid Geometric– Statistical Deformable Model for Automated 3-D Segmentation in Brain MRI. IEEE Trans. Biomed. Eng., vol. 56, pp . 1838-1848, 2009.

[9] Jack Jr., C. R., Knopman, D. S., Jagust, W.J ., Shaw, L. M., Aisen, P. S., Weiner, M.W., Petersen, R. C., Trojanowski, J. Q. Hypothetical model of dynamic biomarkers of the Alzheimer's pathological cascade. Lancet Neurol. vol. 9, pp. 119–128, 2010.

[10] Liew, A. W. C. and Hong Y., "Current methods in automatic tissue segmentation of 3D magnetic resonance brain images," Current Med. Imag. Rev., vol. 2, pp. 91–103, 2006.